

1 Chapter 2

2  
3  
4 **Relations between Climate Variability**  
5 **in the Mediterranean Region and the**  
6 **Tropics: ENSO, South Asian and African**  
7 **Monsoons, Hurricanes and Saharan Dust**  
8  
9  
10

11  
12  
13 Pinhas Alpert,<sup>1</sup> Marina Baldi,<sup>2</sup> Ronny Ilani,<sup>1</sup> Shimon Krichak,<sup>1</sup> Colin Price,<sup>1</sup>  
14 Xavier Rodó,<sup>3</sup> Hadas Saaroni,<sup>1</sup> Baruch Ziv,<sup>4</sup> Pavel Kishcha,<sup>1</sup> Joseph Barkan,<sup>1</sup>  
15 Annarita Mariotti,<sup>5</sup> and Eleni Xoplaki<sup>6</sup>

16 <sup>1</sup>*Tel Aviv University, Israel (pinhas@cyclone.tau.ac.il, saaroni@post.tau.ac.il,*  
17 *shimon@cyclone.tau.ac.il, cprice@flash.tau.ac.il, pavel@cyclone.tau.ac.il)*

18 <sup>2</sup>*IBIMET – CNR, Italy (m.baldi@ibimet.cnr.it)*

19 <sup>3</sup>*ICREA and Climate Research Laboratory, PCB-Univ. of Barcelona, Spain*  
20 *(xrodo@pcb.up.es)*

21 <sup>4</sup>*The Open University of Israel (baruchz@openu.ac.il)*

22 <sup>5</sup>*ENEA, Italy (annarita.mariotti@casaccia.enea.it)*

23 <sup>6</sup>*Institute of Geography and NCCR Climate, University of Bern, Switzerland*  
24 *(elena.xoplaki@giub.unibe.ch)*

25  
26  
27  
28 **2.1. Introduction**  
29  
30

31 The Mediterranean climate is affected by several tropical and subtropical  
32 systems as illustrated by some evidence presented in this chapter. These factors  
33 range from the El Niño Southern Oscillation (ENSO) and tropical hurricanes  
34 to the South Asian Monsoon and Saharan dust. This leads to complex features  
35 in the Mediterranean climate variability. In the following sections, we review  
36 some tropical and subtropical teleconnections to the Mediterranean climate in  
37 the following order: El Niño Southern Oscillation is elaborated in [Section 2.2](#),  
38 the South Asian Monsoon is discussed in [Section 2.3](#), [Section 2.4](#) is dedicated  
39 to African monsoon, tropical cyclones are discussed in [Section 2.5](#) and finally  
40 Red Sea Trough intrusions into the Eastern Mediterranean and the Saharan  
41 dust are discussed respectively in the last two [Sections 2.6 and 2.7](#).

## 2.2. ENSO Impact on the Mediterranean Climate

<sup>1</sup>The El Niño Southern Oscillation (ENSO) phenomenon is recognized as a major source for global climate variability (Halpert and Ropelewski, 1992) either via standing modes over the entire Tropics or via coherent large-scale low-frequency spatial patterns referred to as “teleconnections” over midlatitudes (see Wallace and Gutzler, 1981; Allan et al., 1996; Diaz et al., 2001 for reviews on ENSO).

Several studies have dealt with the underlying physics of the phenomenon and with the worldwide implications for climate (e.g. van Loon and Madden, 1981; Kiladis and Diaz, 1989; Ropelewski and Halpert, 1992; Trenberth et al., 1998; Diaz et al., 2001). The impact of ENSO on the climate of extra-tropical regions, as well as the mechanism responsible for anomalies in the tropical Pacific sea surface temperatures (SST) having worldwide impacts are poorly understood and documented (Pozo-Vázquez et al., 2001).

The El Niño phenomenon is related to the warming of the eastern Pacific sea surface temperatures (SST) for an extended period of 6–12 months, and sometime longer. The SST distribution is directly linked to the atmospheric pressure patterns over the Pacific, with a low pressure cell being located above the warm pool in the western Pacific during normal conditions, while moving eastward with the warm pool in El Niño years. The atmospheric pressure oscillation between the west and central Pacific is known as the Southern Oscillation (SO). Positive pressure anomalies over Australia and Indonesia are associated with the warm El Niño conditions in the eastern Pacific, while negative pressure anomalies over Australia are associated with the cold La Niña conditions in the eastern Pacific. Due to the strong link between the SSTs and the atmospheric pressure, the phenomenon is often referred to as the El Niño/Southern Oscillation.

During warm (El Niño) episodes, the normal patterns of tropical precipitation and atmospheric circulation become disrupted. The abnormally warm waters in the equatorial central and eastern Pacific give rise to enhanced cloudiness and rainfall in that region, especially during the boreal winter and spring seasons. At the same time, rainfall is reduced over Indonesia, Malaysia and northern Australia. Thus, the normal Walker Circulation during winter and spring, which features rising air, cloudiness and rainfall over the region of Indonesia and the western Pacific, and sinking air over the equatorial eastern Pacific, becomes weaker than normal, and for strong warm episodes, it may actually reverse.

The increased heating of the tropical atmosphere over the central and eastern Pacific during warm episodes affects global atmospheric circulation features, such as the jet streams in the subtropics and in the temperate latitudes of the

<sup>1</sup>Much of the preface of this section is based on Xoplaki (2002) and the Climate Prediction Center (CPC) website <http://www.cpc.ncep.noaa.gov/>

AQ: please list the reference.

83 winter hemisphere. The jet streams over the eastern Pacific Ocean are stronger  
84 than normal during warm episodes. Also, during warm episodes, extra-tropical  
85 storms and frontal systems follow paths that are significantly different from  
86 normal, resulting in persistent temperature and precipitation anomalies in many  
87 regions. Significant departures from normal conditions, for the Northern  
88 Hemisphere (NH) winter and summer seasons, can be found at the Climate  
89 Prediction Center (CPC) site: [http://www.cpc.ncep.noaa.gov/products/analysis\\_](http://www.cpc.ncep.noaa.gov/products/analysis_monitoring/lanina/index.html)  
90 [monitoring/lanina/index.html](http://www.cpc.ncep.noaa.gov/products/analysis_monitoring/lanina/index.html)).

91 According to the general descriptions of ENSO above, there is no El Niño/La  
92 Niña impact in either season visible for the European/Mediterranean area.

93 It has been proposed that ENSO exerts a positive forcing on tropical North  
94 Atlantic SSTs and this effect is strongest in boreal spring (Enfield and Mayer,  
95 1997). However, it has been argued that only when tropical SST anomalies are  
96 large (strong ENSO events), the ENSO signal can be found in the extra-tropics  
97 (Huang et al., 1998; Trenberth et al., 1998). On the other hand, tropical forcing is  
98 stronger during the northern winter, coinciding with the mature stage of El Niño  
99 events (Trenberth et al., 1998). It appears that the possible influence of ENSO  
100 in the North Atlantic-European area is more likely to be found during extreme  
101 events of ENSO and during the winter (Pozo-Vázquez et al., 2001). The  
102 perturbation can be propagated downstream, as a wave train, to other longitudes  
103 in the form of Rossby waves, eventually affecting locations far away from the  
104 Pacific, particularly the North Atlantic region. Consequently, the eventual pro-  
105 pagation of such events to other longitudes takes place with a lag of around three  
106 months (Pozo-Vázquez et al., 2001).

107 Several papers have related ENSO to weather and climate variability over  
108 Europe and Africa as well as over specific countries at the Mediterranean Sea  
109 (e.g., Fraedrich and Müller, 1992; Fraedrich, 1994; Rodó et al., 1997; Laita and  
110 Grimalt, 1997; Moron and Ward, 1998; Rodriguez-Puebla et al., 1998; Price  
111 et al., 1998; Türkeş, 1998; Kadioğlu et al., 1999; Rocha, 1999; van Oldenborgh  
112 et al., 2000; Compo et al., 2001; Diaz et al., 2001; Pozo-Vázquez et al., 2001;  
113 Giorgi, 2002; Lloyd-Hughes and Saunders, 2002). A compilation of their findings  
114 together with some others is summarized below.

115

116

### 117 **2.2.1 ENSO and Eastern Mediterranean (EM) Rainfall**

118

119 Yakir et al. (1996) and Price et al. (1998) showed significant connections between  
120 ENSO events and winter rainfall in Israel, both indicate increased rainfall  
121 occurring in El Niño winters. Price et al. (1998) also demonstrated that La Niña  
122 years were associated with below normal rainfall. The 2003–2004 rainy winter  
123 in Israel, coinciding with an El Niño event, supports the above. The analysis

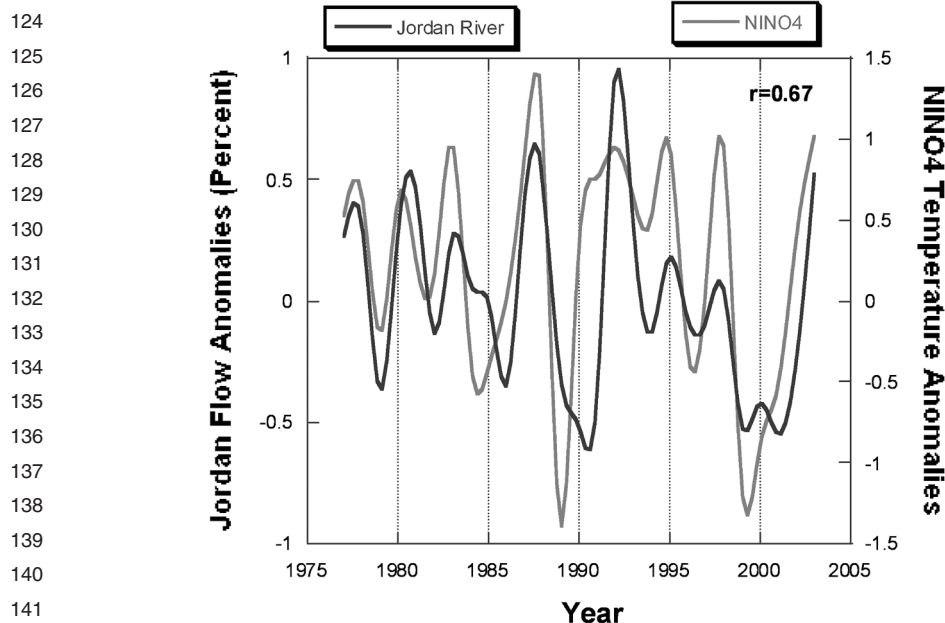


Figure 45: The winter streamflow in the Jordan River and the winter NINO4 SSTs in the tropical Pacific. Adapted from Price et al. (1998).

in Israel was extended to the Jordan River discharge, used as a proxy for regional rainfall, since the stream flow entering the Sea of Galilee is dominated by regional rainfall. The seasonal stream flow in the Jordan River is significantly correlated ( $r \sim 0.67$ ) with the seasonal NINO4 temperatures (Fig. 45). This implies that the tropical Pacific temperature oscillations can explain approximately 45% of the inter-annual variability in winter rainfall in northern Israel. It is hypothesized that the reason for this strong connection is related to the position of the winter jet over the Eastern Mediterranean (EM). Israel is located at  $30^{\circ}\text{N}$ , exactly the mean latitude of the winter jet. Small shifts, in the order of  $\sim 1$  deg, in its mean position can have a major impact on the storm tracks, and hence on the rainfall amounts. Fig 46 shows that indeed in a composite of El-Niño years, the jet over the EM moves further south by about 50–100 km.

During El Niño/La Niña years, meridional shifts of the jet in the EM have been observed. However, the intensity of the ENSO events is not directly related to the intensity of the rainfall anomalies in Israel. This is one of the reasons the correlation coefficient is only 0.67. However El Niño/La Niña years have been wet/dry for 75% of the ENSO events in the last 30 years. Stream flow data in the Jordan River are only available since the end of the 1960s. However,

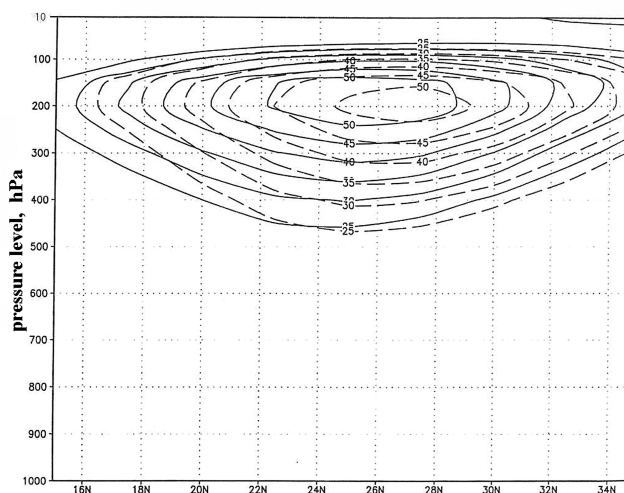


Figure 46: Zonal means ( $30^{\circ}\text{E} - 40^{\circ}\text{E}$ ) of west wind (m/s) in the winter period (December, January and February). The dashed lines correspond to the winters from 1982/83 to 1993/94, while the solid ones, to the El-Niño winters 1982/83, 1986/87 and 1991/92.

since individual rain gauge measurements in the watershed are highly correlated ( $r \sim 0.9$ ) with the catchment's integrated stream flow, it is possible to extend the time series back to 1922. However, the ENSO signal appears in the rainfall/streamflow data only after the mid-1970s. It is puzzling as to why these correlations are observed only in the recent record. This may be a result of the changes in the frequency and intensity of ENSO events since the mid-1970s. Trenberth and Hoar (1997) have shown that since the mid-1970s, there has been a significant increase in the frequency of El Niño events relative to La Niña events, and the intensity and period of these events has also changed. It has also been suggested that there may have been a shift in the global climate system during the 1970s, which may have resulted in a stronger Pacific-mid-latitude link during the past three decades (Wuethrich, 1995).

Kadioğlu et al. (1999) investigated the Turkish monthly total precipitation variation at 108 meteorological stations between 1931 and 1990. They found that much of the month-to-month variability is related to El Niño events. El Niño events, as classified by high ENSO index, seem to produce both depressions and enhancements in the southern and northwestern parts of Turkey, respectively. During El Niño years, the cyclones move towards the north. This may be the reason why there is a decreasing trend in precipitation around the southwest of Turkey (Kadioğlu et al., 1999).

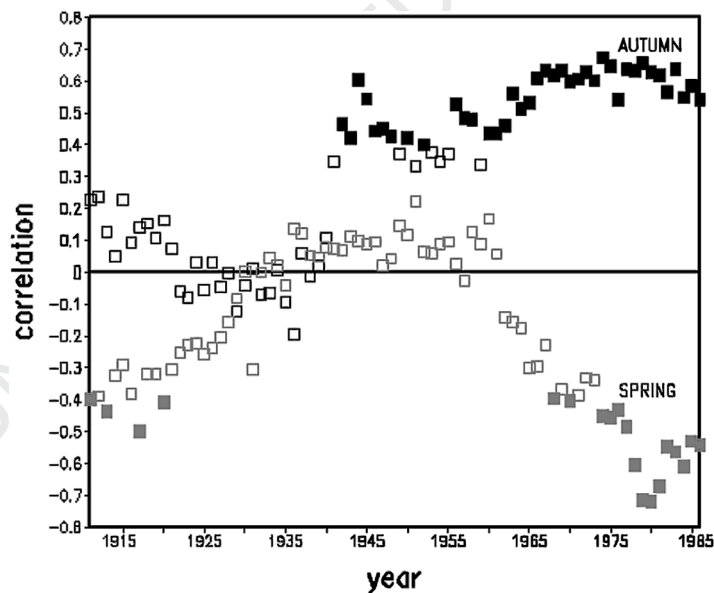
206 **2.2.2 ENSO and the Western Mediterranean Relationship**

207

208 Rodó et al. (1997) investigated the signatures of ENSO in Spanish precipitation  
209 and stated a coherent decrease in March/April/May following El Niño events,  
210 in accordance with that stated in the pioneering studies (Ropelewski and  
211 Halpert 1987, Kiladis and Díaz 1989), and later confirmed and extended by  
212 van Oldenborgh et al. (2000) and Mariotti et al. (2002). This coherence appeared  
213 to increase in the second half of the twentieth century.

214 Mariotti et al. (2002) also found that western Mediterranean-averaged  
215 rainfall is significantly correlated with ENSO variability during autumn, with  
216 the sign being opposite to that found in spring. A composite analysis reveals an  
217 approximate 10% increase (decrease) in seasonal rainfall for El Niño (La Niña)  
218 events in September/October/November, preceding the mature phase of ENSO,  
219 with an early (late) arrival of the rainy season in these regions. This relationship  
220 appears to have been stationary starting from the late 1940s (Fig. 47).

221 Mariotti et al. (2005) investigate the Mediterranean autumn ENSO-signal  
222 in the context of the impact that ENSO events have on a larger domain extending  
223 from southwest Europe/ northern Africa into parts of southwest Asia, as also  
224



225  
226  
227  
228  
229  
230  
231  
232  
233  
234  
235  
236  
237  
238  
239  
240  
241  
242 Figure 47: Correlations between western Mediterranean rainfall (from the data  
243 base of the Climate Research Unit (CRU), University of East Anglia, UK) and  
244 Niño3.4 indices in autumn (SON, black) and spring (MAM, grey). Each value  
245 refers to the correlation in a 20-year window centered at the symbol. Full symbols  
246 are for values at least 95% significant (After Mariotti et al., 2002, Fig. 6 therein).

## ARTICLE IN PRESS

247 found by the early work of Kiladis and Díaz (1989) and Mason and Goddard  
248 (2001). The observational evidence suggests a link between southwest Europe  
249 rainfall anomalies and circulation anomalies in the North Atlantic/European  
250 sector, while a more direct connection to the Indo-Pacific region and  
251 Middle-Eastern jet-stream variability for the rainfall anomalies in southwest  
252 Asia. The teleconnection mechanisms for warm and cold ENSO events appear  
253 to be different, with a prevailing signature of PNA/NAO-like variability in the  
254 former case and a more relevant role for tropical Atlantic SST anomalies in  
255 the latter (Fig. 48).

256 Regarding ENSO signatures in the North Atlantic/European sector by  
257 using common statistical techniques, Rodó (2001) highlighted the difficulty  
258 in isolating ENSO signals mainly due to their spiky nature with respect to  
259 the dominating mid-latitude dynamics. Their importance for the Mediterranean  
260 climate might be high, though only for selected intervals and vanish elsewhere.  
261 Rodó (2001) showed this occurrence for SST anomalies in the western  
262 Mediterranean basin. The possibility of an ENSO influence through perturba-  
263 tions of the Atlantic Walker circulation was also highlighted by Rodó (2001),  
264 who stated the importance of a weak Atlantic Hadley cell as a response to  
265 anomalous warming in the eastern tropical Pacific. This is in accordance with  
266 Sutton et al. (2000), Saravanan and Chang (2000) whose results suggest that  
267 a fraction of the inter-hemispheric variability in the tropical Atlantic is forced  
268 by way of a tropical atmospheric bridge (Lau and Nath, 1996, Klein et al., 1999).

269 Correlation between ENSO and Iberian rainfall has increased in the second  
270 half of the 20th century (Rodó et al., 1997), but the only relevant (significant)  
271 area is confined to the eastern part of the peninsula. Later studies confirm  
272 these connections and suggested possible mechanisms responsible for those

273

274

275

276

277

278

279

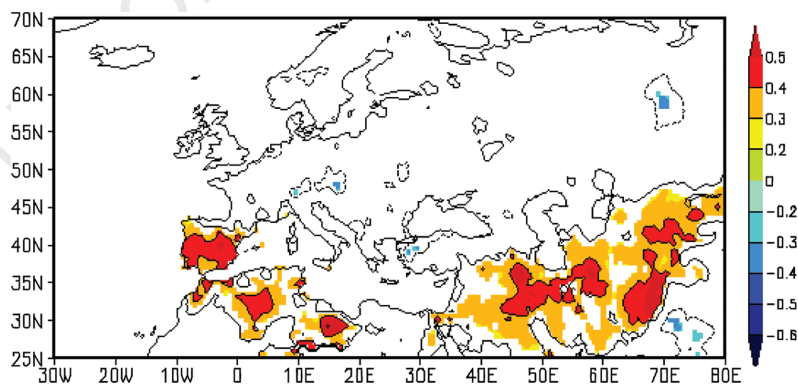
280

281

282

283

284



285

286

287

Figure 48: Correlations between Euro-Asian autumn rainfall and Nino3.4 indices for the period 1948–2000. Shading depict region where the correlation is at least 95% significant. Data is from CRU. (After Mariotti et al., 2005, Fig. 1a therein).

288 associations (Rodó, 2001; van Oldenborgh et al., 2000; Mariotti et al., 2002),  
289 which appear to involve a typical bipolar seesaw between the Mediterranean  
290 region and northern Europe.

291 Correlations between ENSO and Iberian rainfall are maximum in autumn  
292 before a mature El Niño phase and in the spring following the El Niño peak.  
293 Sign of the correlations points to an increase in autumn rainfall in the year 0  
294 and a decrease in spring precipitation in the year + 1.

295 ENSO-Iberian rainfall correlations may account for up to 50% of springtime  
296 decrease in rainfall in certain areas while slightly lower values, showing a converse  
297 association with El Niño, were estimated for autumn. These values mostly  
298 concentrated in the second half of the last century, a time when correlations  
299 appear to have intensified (Rodó et al., 1997; Mariotti et al., 2002), particularly  
300 after the 1960's.

301 The ENSO influence appears most relevant at inter-annual timescales than  
302 the NAO effect. At inter-annual timescales the NAO effect shows no clear  
303 signature on Iberian rainfall, except for small selected areas. Conversely, ENSO  
304 accounts for half of the total annual variance in southeast Spain and parts  
305 of Morocco. The potential for future predictability needs to be further assessed  
306 in the light of the lack of current predictors for Mediterranean climate at  
307 inter-annual timescales and provided there is a sufficient time lag of some months  
308 between the two processes here involved. A gain of the inter-annual predictability  
309 potential would be mostly relevant for agricultural systems and other economic  
310 activities with the high impact on population in the Mediterranean region  
311 (Rodó and Comín, 2000)

312

313

### 2.2.3 *ENSO and Extreme Mediterranean Rainfall*

314

315

316

317

318

319

320

321

322

323

324

325

### 2.2.4 *Transient and Stationary Waves Approach*

326

327

328

Previous work has shown an ENSO-impact during boreal winters, with a trough  
(ridge) over southern Europe during El Niño (La Niña) events, accompanied

329 by more (less) cyclones reaching the Mediterranean region. That is, both the  
330 mean flow and the sub-seasonal variations of the flow are affected by ENSO.  
331 In particular, the sub-seasonal variations tend to feedback on the anomalous  
332 mean flow. However, the impact in the Atlantic and Europe, and, in particular,  
333 in the Mediterranean region, appears to be more robust during La Niña  
334 events than during El Niño ones. Previous work from the Interannual and  
335 Decadal Climate Variability: Scale Interaction Experiments (SINTEX) EU  
336 project (Gualdi et al., 2003) indicated that the dominating mode of interaction  
337 – resembling the NAO – is only related to La Niña but not to El Niño events.  
338 Further, these modes – though defined in the Atlantic and Europe – appear to  
339 be connected to the North Pacific and North America. This suggests that  
340 transient eddies are also important in “transporting” the ENSO-response from  
341 the latter regions to the Atlantic and Europe. This insight gained may improve  
342 the prospects of seasonal prediction in the Atlantic/European region. Modelling  
343 experiments could cope with a complex response to ENSO through the alteration  
344 of mid-latitude internal modes of variability (e.g., NAO, East Atlantic/West  
345 Russian (EATL-WRUS), etc.), in particular with respect to future scenarios (e.g.  
346 Timmermann et al., 1999).

347

348

### 349 *2.2.5 Possible Coupling Mechanism of ENSO and the Mediterranean*

350

351 The search for the physical mechanisms that might be responsible for the  
352 connection between the tropical Pacific and the North Atlantic European region  
353 was initiated through the exploration of ENSO signatures in different regions of  
354 the tropical Atlantic. Lanzante (1996) and Enfield and Mayer (1997) explored  
355 remote forcing of the tropical Atlantic and noted a significant correlation with  
356 ENSO. They suggested that a fraction of the inter-hemispheric variability in the  
357 tropical Atlantic is forced by way of a tropical atmospheric bridge (Lau and  
358 Nath, 1996; Klein et al., 1999). Other studies have suggested such a link along a  
359 zone from 10°N to 20°N (Curtis and Hastenrath, 1995; Nobre and Shukla, 1996;  
360 Mestas-Núñez and Enfield, 2001). In addition, Sutton et al. (2000) and  
361 Saravanan and Chang (2000) suggest an influence through perturbation of the  
362 Atlantic Walker circulation. This possibility was also highlighted by Mestas-  
363 Núñez and Enfield (2001) and Rodó (2001), who stated the importance of a weak  
364 Atlantic Hadley cell as a response to anomalous warming in the eastern tropical  
365 Pacific. Finally, Sutton et al. (2000) suggested that a variety of competing  
366 mechanisms might be responsible for the weakening of the Atlantic cell during  
367 boreal winters. Recently, Ruiz-Barradas et al. (2003) with the aid of model  
368 simulations and the NCEP–NCAR reanalysis data for the period from 1958  
369 to 1993, showed how anomalous ENSO-related diabatic heating influences

370 near-surface winds in the tropical Atlantic. This remote influence directly induces  
371 changes in the intensity of both the Atlantic Walker and Hadley circulations.

372 The simulation of Mediterranean climate as influenced by some major modes  
373 of atmospheric variability appears to have improved in the recent years (see also  
374 Luterbacher et al., this book; Trigo et al., this book). In particular, the simula-  
375 tion of NAO responses to ENSO was improved. However, the nature of NAO  
376 prospects for predictability are limited to a few months and do not offer much  
377 field for predictability studies in the seasonal/interannual range. In this respect,  
378 a notable portion of the NAO predictability potential for future studies lies  
379 at scales longer than decades (Griffies and Bryan, 1997).

380 Several reasons may account for the limited ability of the GCM to simulate the  
381 ENSO responses at mid-latitudes. Among those, note, for instance:

- 382 • ENSO transmission to mid-latitudes appears to operate through a complex  
383 teleconnection pattern that interacts with strong internal mid-latitude atmo-  
384 spheric dynamics. This transition further complicates its observational  
385 identification with techniques that need study of aggregates or “composite”  
386 events. This fact may also result in a serious limitation of its predictability  
387 potential. For instance, occasionally different events have been documented to  
388 have yielded different responses.
- 389 • The coarse resolution of global models over the Mediterranean region does not  
390 yet yield credible simulation scenarios.
- 391 • The nesting of regional models in global models is not yet developed enough  
392 for the Mediterranean sector, though together with downscaling techniques  
393 provides a promising area to investigate in the future.
- 394 • The Mediterranean sea is not adequately integrated in most model simulations.  
395 In addition, boundary responses coming from adjacent oceanic and terrestrial  
396 regions surrounding the Mediterranean area are not fully covered in regional  
397 experiments, yielding a poor representation of Mediterranean conditions.
- 398 • Processes of the previous four items may be responsible for some difference  
399 in ENSO sensitivity detected by observational and modelling studies. The  
400 latter usually yields weaker responses to ENSO out of the tropical regions  
401 (Rodó, 2001). A deficient integration of transients and transitory couplings  
402 might account for a significant portion of the residual variability left, as proved  
403 by recent observational studies.

404  
405 Recent modelling studies show new areas for exploration in ENSO telecon-  
406 nections, which might be of use in the future, in the search for increasing  
407 predictability of the Mediterranean climate. This is, for instance, the case  
408 with experiments seeking to simulate the atmospheric forcing in regions of the  
409 tropical North Atlantic during ENSO events (Lau and Nath, 2001). Another  
410 possibility is increasing horizontal resolution to obtain more reliable responses.

411 This is the case for a recent study by [Merkel and Latif \(2002\)](#), illustrating that an  
412 increase of the horizontal resolution (from T42 to T106) causes significant  
413 changes in sea level pressure (SLP), temperature and precipitation over the  
414 Mediterranean as well as in the transient/ stationary wave activity. A southward  
415 shift of the North Atlantic low pressure systems in the winter season during  
416 El Niño was also noticed.

417

418

### 419 **2.3. South Asian Monsoon Variability and the** 420 **Mediterranean Climate**

421

422 The South Asia Monsoon (SAM) is a key factor influencing the climate of the  
423 eastern and central Mediterranean ([Reddaway and Bigg, 1996](#); [Rodwell and](#)  
424 [Hoskins, 1996](#), [Ziv et al., 2004a, b](#)). It causes high variability in SLP over Arabia  
425 and the Middle East with high pressures in winter and low pressures in summer.  
426 The adjustment to the SAM couples the falling pressure and land temperature  
427 over the Indian subcontinent/ Asia Minor, with rising pressure and temperature  
428 over the Persian Gulf and Iraq.

429 Another possible explanation for the different climatic behaviour of the eastern  
430 and western Mediterranean basins is derived from the gradual delay, of up to  
431 two weeks, of the onset of the monsoon in the 1980s, as compared with that  
432 in the early 1950s ([Subbaramayya et al., 1990](#)). This places the period of monsoon  
433 low pressure firmly in the summer months (JJA), whereas, previously, it  
434 was partly in May. On an average, this potentially lowers the summer pressure  
435 along with the temperature by shifting the monsoonal cloud cover, later in  
436 the season ([Reddaway and Bigg, 1996](#)). In accordance with [Kripalani and](#)  
437 [Kulkarni \(1999\)](#), this monsoonal delay could be attributed to the prolonga-  
438 tion of the winter snow cover over Eurasia. They reported on a significant  
439 negative (positive) relationship between the wintertime snow depth over western  
440 Eurasia (eastern Eurasia and central Siberia) and subsequent Indian monsoon  
441 rainfall. This correlation structure is indicative of a mid-latitude longwave  
442 pattern with an anomalous ridge (trough) over Asia, during the winter prior to  
443 a strong (weak) monsoon.

444 [Rodwell and Hoskins \(1996\)](#) showed that the Asian Summer Monsoon domi-  
445 nates not only Central Asia, but also the Eastern Mediterranean (EM). By  
446 using numerical simulations, they pointed at the linkage between the appearance  
447 of the semi-permanent subsidence structure over the EM and the onset of the  
448 Monsoon. The climatic regime and the dynamic factors governing the EM in the  
449 summer season, and their relationships with the Asian Monsoon, were analyzed  
450 by [Ziv et al. \(2004a\)](#), who found significant correlation on the interdiurnal  
451 time-scale. They identified a circulation connecting the upward motion maximum

AQ: please clarify whether it is OK as edited? (2004a,b instead of 2004)

452 over the Himalayas with the downward motion over the EM. Raicich et al. (2003)  
453 studied the relationship between the Asian and African Monsoon systems  
454 and found a high correlation between the intensity of each of them and the  
455 pressure distribution over the Mediterranean on the interannual time-scale.

456 The monsoon–desert mechanism presented by Rodwell and Hoskins (1996)  
457 may not be confined to the Asian monsoon alone. In a similar way, it could  
458 explain the relationship between the observed summertime strengthening of  
459 the oceanic sub-tropical anticyclones and the existence of western continental  
460 deserts and of “Mediterranean type” climate regions. They showed that the  
461 monsoon could force a remote descent to its west and northwest. The very dry  
462 summertime climate of the Mediterranean and the surrounding lands may be  
463 strongly related to this. They also showed that this descent is highly dependent  
464 on the latitude of the monsoon heating; a southward shift, for example, may  
465 lead to wetter weather, for southern Europe.  
466

467

### 468 ***2.3.1. Mediterranean Climate and South Asian Rainfall***

469

470 The Indian summer Monsoon index has been recorded for almost 200 years,  
471 while records of the subsequent winter rain in Israel are relatively “younger”;  
472 the longest record used is the one kept in Jerusalem, for the past 118 years.  
473 The overall correlation between these two indices was found to be only  $-0.3$  (for  
474 the past 118 years). However, in 73 years (62%), the indices sign were the  
475 opposite. For extreme summer seasons, in which the index deviates by over  
476 1.3 standard deviations, the correlation increases to  $-0.56$  (Alpert et al., 2003).  
477 Similar results were found for other relatively long-record of rainfall stations  
478 in Israel. This illustrates the potential of the Indian Monsoon as a predictor  
479 for Israeli rainfall in the subsequent winter season.

480 An important index of monsoon precipitation is the All-India Rainfall  
481 Index (AIR; Parthasarathy et al., 1995). It is an areal average of rainfall for  
482 29 sub-divisions, which come from areally averaged district rainfalls. Rainfall  
483 amounts are totals for June, July, August and September (Parthasarathy et al.,  
484 1995). The AIR data are available online at: <http://grads.iges.org/india/allindia.html>. Liu and Yanai (2001) found significant positive correlation  
485 between June–September AIR and JJAS tropospheric temperature from 1949  
486 to 1998, over the entire Mediterranean and northern Africa, within pressure  
487 levels from 200 and 500 hPa levels. Similar results have been revealed for the  
488 southern and eastern Mediterranean in June and for the eastern Mediterranean  
489 in August (Liu and Yanai, 2001).  
490

491 While the role of the Tropical Atlantic Variability (TAV), ENSO and  
492 associated changes in SST over the tropical Pacific and Atlantic oceans have

493 been widely investigated, the effect of the Indian Ocean on monsoon rainfall  
494 is not well understood. The existence of the Indian Ocean Dipole (IOD) mode  
495 was demonstrated by Saji et al. (1999) Webster et al. (1999) and Andersen (1999).  
496 A respective index was determined, though no statistical relationship between  
497 the index and the monsoon rains has been established. It is suggested that  
498 the variations in distribution and intensity of the EM rainfall, during the last  
499 decade, are associated with variations in the characteristics of the air mass over  
500 the Indian Ocean via its transport toward the EM. However, recent findings of  
501 idealized SST anomaly experiments by Hoerling et al. (2004) and Hurrell et al.  
502 (2004), indicate that SST variations have significantly controlled the North  
503 Atlantic circulation, related to the NAO, with the warming of the tropical Indian  
504 and western Pacific Ocean being of particular importance.

505 When the winter regime over the entire Mediterranean is considered, the  
506 focus is given to the Rossby waves and other extra-tropical factors (such as the  
507 NAO) as the dominating features. However, some attention should be given  
508 to continental polar outbreaks associated with the South Asian Monsoon  
509 (e.g. Saaroni et al., 1996).

510

511

#### 512 **2.4. African Monsoon Impact on the Climate** 513 **of the Mediterranean**

514

515 The climatic variables in the various parts of the Mediterranean are corre-  
516 lated with each other as well as with external circulations. For instance, the  
517 Mediterranean SLP oscillation (MO), i.e., the difference between its western and  
518 eastern parts, is correlated with precipitation. In winter, a fundamental role  
519 is played by the NAO index, whereas in summer, the regional Hadley cell was  
520 found to be correlated with climatic conditions over parts of the Mediterranean  
521 (see Trigo et al., this book). There is also some evidence for teleconnections with  
522 the South Asian Monsoon and with the Sahel precipitation. The correlation  
523 between the precipitation indices of these two systems and the MO is negative  
524 over the EM and positive over the western Mediterranean. The relevant govern-  
525 ing mechanisms have been studied by several authors (see Baldi et al., 2002  
526 for an extended bibliography), as well as the influence of the position and the  
527 strength of the Hadley cell (Dima and Wallace, 2003).

528 Focusing on the summer season, Chen et al. (2002), showed evidence  
529 for strengthening of the tropical general circulation in the 1990s, and in parti-  
530 cular the West Africa monsoon, reaching its northernmost extension in August,  
531 when the ITCZ, after the abrupt shift at the end of June and further slow  
532 northward migration, reaches its northernmost location (Sultan and Janicot,  
533 2000, 2003). Important mechanisms, such as heat and moisture advection in

534 North America and Asia and anomalously high values of the surface albedo in  
535 northern Africa, limit a further extension towards northern latitudes (Chou and  
536 Neelin, 2003; Rodwell and Hoskins 1996, 2001). The two regimes, the dry and hot  
537 summers in the Mediterranean and the monsoon regime over West Africa, are  
538 highly correlated; interactions and feedback mechanisms between the two are not  
539 only possible, but also evident (Rowell 2003, Baldi et al., 2002, 2003a, b).

540 Ziv et al. (2004a), in their study of the summer regime, found a signature of the  
541 Hadley cell over eastern North Africa, connecting the EM with the African  
542 Monsoon. The relationship between them is manifested by a significant correla-  
543 tion between the ascent at 15°N –20°N latitudes and the descent at 30°N –40°N  
544 latitudes. The correlation between the EM subsidence and the Asian Monsoon  
545 was further validated through correlating the inter-diurnal variations of the  
546 vertical velocities of the two Monsoon systems, yielding  $r=0.33$ , in spite of the  
547 ~6000 km distance.

548  
549

## 550 **2.5. Tropical Cyclones' Impact on the Mediterranean Climate**

551

552 Reale et al. (2001) showed that several cases of severe floods over the western  
553 Mediterranean could be traced back to hurricanes. Also, Hoskins and Berrisford  
554 (1988) related the severe 1987 storm in South England to hurricanes. Next,  
555 we review a first study showing the relationship between flooding in Israel  
556 and hurricanes (Fig. 49). Over the period from 3–5 December, 2001, there were  
557 heavy rains in northern Israel reaching 250 mm in some areas. The rains were  
558 associated with a relatively weak cyclone system approaching the area from  
559 the north-west. Atmospheric developments that produced the unusually intense  
560 rainfall and flash floods in Israel during 3–5 December 2001 were associated  
561 with upper-tropospheric jet stream activity. This activity was stimulated by  
562 the potential vorticity (PV) streamer conditions in the upper troposphere and  
563 by the intense intrusion of cold stratospheric air masses into the troposphere  
564 over the Mediterranean Sea area. Local topography and geography of the EM  
565 region also played a role of an additional triggering factor in the process. The  
566 intense synoptic processes of December 2001 were initiated by the development  
567 of a tropical storm, which subsequently developed into hurricane Olga (from  
568 25 to 29 November) accompanied by intense ascent motions in the tropical  
569 Atlantic. Convergence of huge amounts of atmospheric water vapour took place  
570 during the first stage of the hurricane development. Both the rise of large  
571 amounts of warm and moist tropical air and the subsequent release of latent heat  
572 caused an additional intensification of the hurricane.

573 This process also induced development of an anticyclone to the north-east of  
574 Olga. The ascending moist air from Olga was later transported to Europe and

575  
576  
577  
578  
579  
580  
581  
582  
583  
584  
585  
586  
587  
588  
589  
590  
591  
592  
593  
594  
595  
596

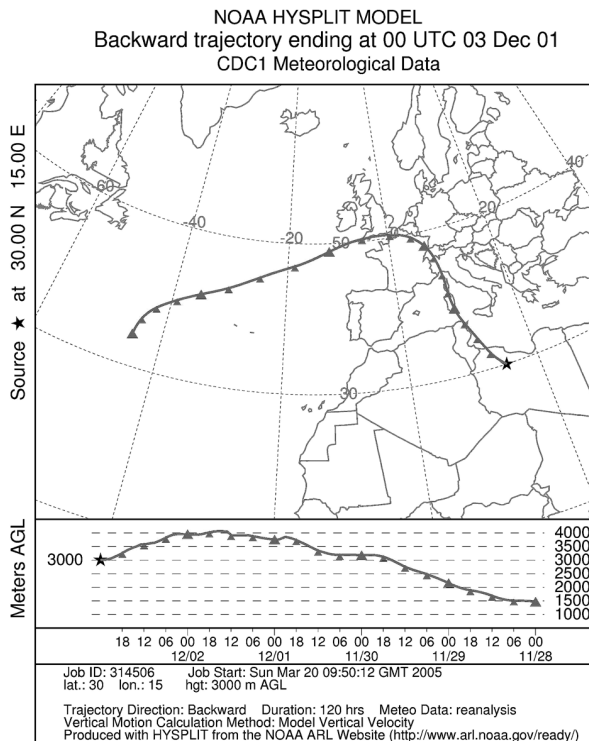


Figure 49: The back-trajectory from Mediterranean to Hurricane Olga3 - **December** - - > 28 November 2001.

AQ: Please clarify if it is 2 december instead of just December

601 finally to the Mediterranean region by the high intense clockwise atmospheric  
602 circulation in the process of Olga's decline. This process led to the southward  
603 propagation of the polar jet and to the establishment of a situation characterized  
604 by the tropopause fold PV streamer with an extrusion of cold upper-tropospheric  
605 and stratospheric air over the south Alpine and the central Mediterranean  
606 areas. Formation and intensification of the EM cyclone of 3–5 December 2001  
607 was additionally stimulated by the interaction of the polar and subtropical  
608 jets over the region (Krichak et al., 2004).

609  
610

## 611 2.6. Tropical Intrusions into the Mediterranean Basin

612  
613  
614  
615

Rains in the Mediterranean basin take place mainly during winter, most of which is associated with Mediterranean baroclinic cyclones. Winter Mediterranean cyclones have their origin in the North Atlantic synoptic systems,

616 in secondary lows formed when upper troughs interact with local orography,  
617 and/or with low level baroclinicity over the northern Mediterranean coast.  
618 However, processes originating from tropical regime are also significant in its  
619 eastern part (Krichak et al., 1997a,b; Krichak and Alpert 1998; Dayan et al.,  
620 2001; Kahana et al., 2002; Ziv et al., 2004b) and along its western part, in north  
621 western Africa (Knippertz et al., 2003). The Red Sea Trough (RST) is one  
622 of the impressive manifestations of mid-latitude–tropical interactions in the  
623 EM especially during autumn and spring. The intensity and duration of the EM  
624 rain-spells highly depend on the interactions between the upper and lower-  
625 tropospheric jets as well as their positioning and orientation. Specific jet  
626 characteristics stimulate development of meso-scale convective complexes and  
627 cyclogenesis. Due to turbulence associated with strong wind shear, tropopause  
628 folding may allow intrusions of the stratospheric air into the troposphere.  
629 It was recently shown that frequencies of RST intrusions to the EM, have  
630 nearly doubled since 1970 from about 50 d/y to about 100 d/y (Fig. 50) (Alpert  
631 et al., 2004a,b)

632 Another type of rainstorms originating from the tropics is associated with  
633 “tropical plumes”. This is a long cloud band that extends from the ITCZ down  
634 to 30°N–40°N latitude, accompanied by a pronounced trough in the Subtropical  
635 Jet to its west combined with a ridge to the east, while no common distinct system  
636

637

638

639

640

641

642

643

644

645

646

647

648

649

650

651

652

653

654

655

656

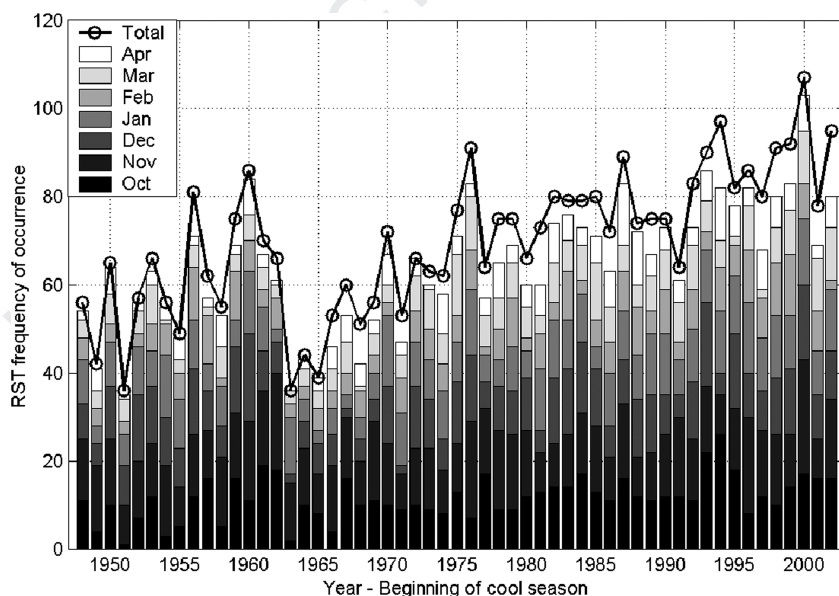


Figure 50: The Red Sea Trough frequencies as totals per hydrological year (August to July) and cumulative monthly contributions (October to April).

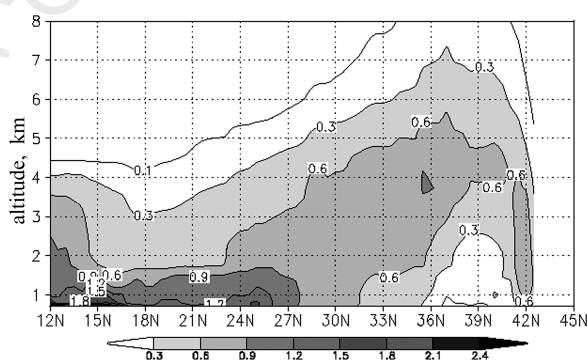
657 at the surface or at the 500hPa level, was found. Ziv (2001) found that prior  
658 to such type of a rainstorm the “tropical plume” is generated. It extends toward  
659 the subtropics, injects moisture of tropical origin that is captured by the  
660 Subtropical Jet, and if a pronounced trough develops there, extensive stratified  
661 cloudiness and widespread rains result. Zangvil and Isakson (1995) found in a  
662 rainstorm of the same type that the vertically integrated moisture convergence  
663 reached  $1.8 \text{ mmh}^{-1}$  over Israel, mostly above the 750 hPa level. Dayan and  
664 Abramski (1983) found an abnormal feature in the Subtropical Jet structure,  
665 i.e. a reversed position of its axis that leads to the formation of a large  
666 and humid warm air mass up to very high levels in the atmosphere above the  
667 Middle East.

AQ: please list  
the reference

## 2.7. Mediterranean Dust Transport from Sahara

672 The role of atmospheric aerosols on the climate system is found to be most  
673 significant (IPCC, 2001). The dust radiative effect strongly depends on its vertical  
674 location. Daily model-based forecasts of 3D-dust fields could be used in order  
675 to determine the dust radiative effect in climate models, because of the large  
676 gaps in observations of dust vertical profiles (Alpert et al., 2004c). The averaged  
677 dust vertical distribution, based on the 3-year database of 48-hour dust forecasts,  
678 shows significant differences between the Atlantic and the Mediterranean  
679 dust transport. As a whole, the Mediterranean dust is found to be within  
680 a wider range of altitudes, penetrating high into the troposphere (Fig. 51).

681 Supporting evidence for this characteristic feature of the Mediterranean  
682 dust transport was obtained from the analysis of lidar dust profiles over Rome



695 Figure 51: Latitudinal cross-sections of averaged dust concentrations  
696 ( $10^{-7} \text{ kg/m}^3$ ) for the months of April, zonal averaged within the longitudinal  
697 zone  $30^\circ\text{E}$ – $40^\circ\text{E}$ . Adapted from Alpert et al. (2004c).

698 (Italy), collected in the 3-year period 2001–2003 during the high dust activity  
699 season from March to June (Kishcha et al., 2005). Based on the data set of dust-  
700 affected lidar profiles (206), Fig. 52 presents histograms of the main parameters  
701 of these dust layers. In particular, the bottom boundary was found to range from  
702 0.5 to 5 km, with the mean value  $BT = 1.6 \pm 0.8$  km; the top boundary ranges  
703 from 2.4 to 8 km, with mean value  $TP = 5.1 \pm 1.1$  km, and the thickness of dust  
704 layers ranges from 0.4 to 7.5 km, with mean value  $TH = 3.6 \pm 1.5$  km. Hence, on  
705 an average, dust over Rome is distant from the surface and penetrates high into  
706 the troposphere. Moreover, as shown in Fig. 52, the Gaussian fitting curves suit  
707 the histograms of lidar-derived data. In seasons other than March – June, some  
708 indication of the mean vertical distribution of dust over Rome can be found  
709 in Gobbi et al. (2004), based on lidar data collected in the year 2001.

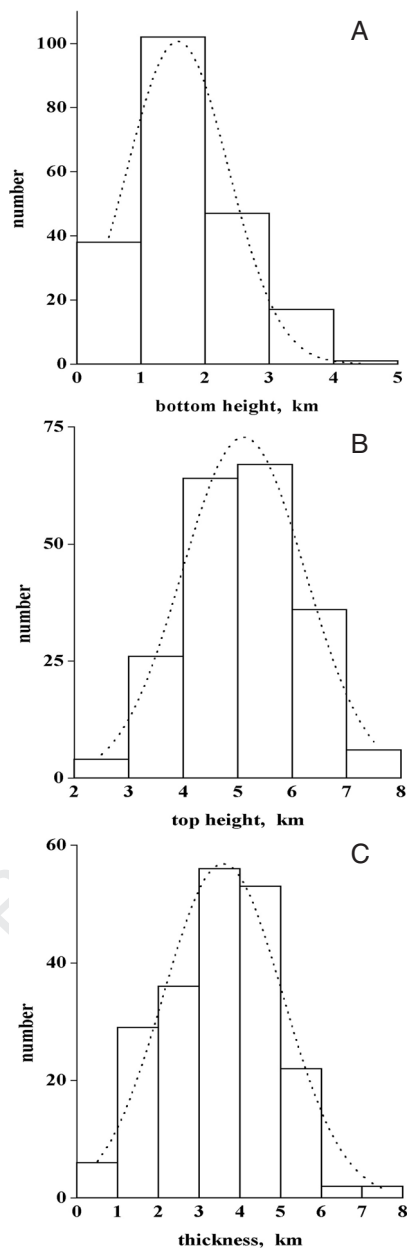
710 The lidar vertical profiles collected in the presence of dust over Rome were  
711 also used in order to validate the TAU dust model. A quantitative comparison  
712 of model vertical profiles against lidar soundings was made and the model was  
713 found good in about 70% of the cases (Kishcha et al., 2005).

714 Saharan dust is generally transported over the Mediterranean by southerly  
715 winds generated by cyclones (Alpert and Ziv, 1989; Bergametti et al., 1989;  
716 Alpert et al., 1990; Moulin et al., 1998). In particular, Alpert and Ziv (1989)  
717 found that spring and early summer are the most favourable periods for the  
718 development of Saharan lows (also called Sharav cyclones) south of the Atlas  
719 Mountains. Usually, such cyclones move eastward and cross Egypt, Israel and  
720 the eastern Mediterranean basin. As shown by Bergametti et al. (1989) and  
721 Moulin et al. (1998), dust outbreaks to the western and central parts of the  
722 Mediterranean are linked with two depression centres: Saharan lows and a high  
723 over Libya. The high over Libya prevents Saharan lows from following  
724 an eastward direction. This synoptic situation, having a peak in spring and  
725 in early summer, induces strong south and southwestern winds between the  
726 two systems and is characterized by dust intrusions from North Africa to the  
727 Mediterranean basin. Moreover, complex wind fields associated with frontal  
728 zones under those atmospheric conditions could be one of the causal factors  
729 for dust over the Mediterranean being within a wide range of altitudes,  
730 penetrating high into the troposphere, as mentioned above.

731 The mean synoptic situation associated with dust outbreaks from Sahara  
732 into the central Mediterranean was examined on a daily basis for the month  
733 of July from 1979 to 1992 (Barkan et al., 2004). It was found that the strength  
734 and position of two essential features of the circulation patterns, such as  
735 the trough emanating southward from the Iceland low and the eastern cell  
736 of the subtropical high, are the governing factors in making suitable flows for  
737 the Saharan dust transportation toward Central Europe. The typical composite  
738 pattern of wind in the case of five days of great quantity of dust in the atmosphere

AQ: please  
list the  
reference.

739  
740  
741  
742  
743  
744  
745  
746  
747  
748  
749  
750  
751  
752  
753  
754  
755  
756  
757  
758  
759  
760  
761  
762  
763  
764  
765  
766  
767  
768  
769  
770  
771  
772  
773  
774



775 Figure 52: Statistical distributions of lidar-derived parameters of the dust layer  
776 over Rome from March to June based on the data set of dust-affected lidar profiles  
777 (206) between 2001 and 2003: bottom (A) and top (B) heights (km), and thickness,  
778 km (C). Fitting curves of the Gaussian distribution are shown by dotted lines.  
779 From Kishcha et al. (2005).

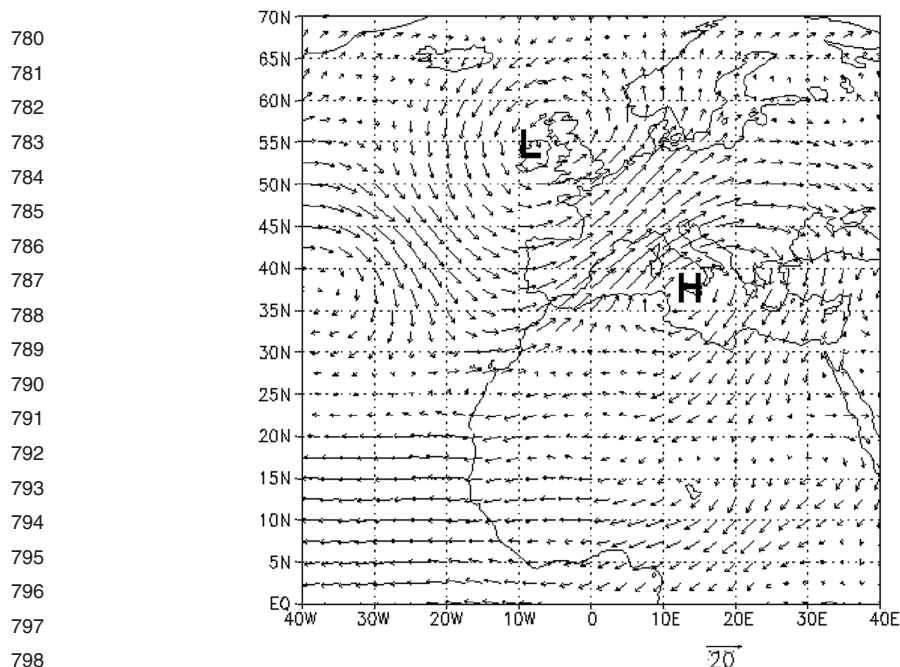


Figure 53: Average wind flow of the dusty period 5–9 July 1988 at 700 hPa. Adapted from Barkan et al. (2005).

above Italy between 5 and 9 July 1988 is shown in Fig. 53. A deep low over Ireland with a strong trough emanating from it southward and splitting the subtropical high into two separate cells is apparent. The eastern high pressure centre is located over Sicily. Between the Irish low and the Sicilian high, a strong southwesterly flow transports dust from Mauritania across the western Mediterranean to central Europe.

## 2.8. Conclusions and Outlook

The aforementioned evidence of tropical teleconnections to the Mediterranean climate suggests further analysis in order to test these relationships by using appropriate modelling and statistical methodologies. The factor separation method (Stein and Alpert, 1993; Alpert et al., 1995) may be useful for distinguishing among contributions of several factors and also of their synergistic effects in producing weather patterns over the Mediterranean. Thus, the modelling approach with a well-defined methodology is necessary for a

AQ: please list the reference

821 clear and simple mechanistic understanding of the different teleconnections  
822 discussed here.

823

824

### 825 ***2.8.1. Future Research on ENSO Impact on Mediterranean Climate***

826

- 827 ● Investigate the role of mid-latitude ocean in responding to the atmospheric  
828 forcing which have a tropical origin (Lau and Nath, 2001) and its effect on  
829 the Mediterranean climate.
- 830 ● Improve resolution and accuracy of observational studies with the use of  
831 a denser, homogeneous set of instrumental records.
- 832 ● Implement new statistical techniques capable of address local phenomena.  
833 These are needed to address ENSO and other tropical influences in the  
834 Mediterranean climate. As an example, the new Scale-Dependent Correlation  
835 (SDC) technique (Rodó, 2001, Rodó et al., 2002, Rodríguez-Arias and Rodó,  
836 2003) may be useful.
- 837 ● Analyse and devise modelling experiments which can cope with a complex  
838 response to ENSO, also through the alteration of internal modes of variability  
839 at mid-latitudes (e.g., NAO, EATL-WRUS, etc.).
- 840 ● Improve the nesting of regional climate models, increase their horizontal  
841 resolution and refine model simulations for a more realistic representation  
842 of the Mediterranean climate.
- 843 ● Explore the different scenarios of the future ENSO frequency and intensity  
844 changes, in response to climate change (e.g. Timmermann et al., 1999). Assess  
845 their relation to the Mediterranean climate variability and extremes.

846

847

848

### 849 ***2.8.2 Future Research on South Asian Monsoon Variability***

850

851

- 852 ● To study teleconnections of the South Asian Monsoon with the eastern  
853 Mediterranean for different time scales, i.e. interannual, seasonal and decadal  
854 time scales. Attempt to evaluate the range of influence of the Asian Monsoon  
855 over the entire Mediterranean basin.
- 856 ● To study long-term trends of various variables, as Saaroni et al. (2003)  
857 performed for summer temperature, in relation to long-term trends in the  
858 South Asian Monsoon features along the entire year.
- 859 ● To study the detailed structure of summer circulations over the eastern  
860 Mediterranean region prior to and during extreme episodes in which the EM  
861 undergoes heat waves or exceptional rain events.

- 862 ● To incorporate data about the South Asian Monsoon into the seasonal  
863 prediction scheme for the Israel winter rainfall.  
864 ● To validate the suggested linkages between the Indian Ocean processes and  
865 the eastern Mediterranean climate.  
866 ● To develop a climatologic basis for continental polar outbreaks events  
867 over the Mediterranean. This includes both synoptic and statistical detailed  
868 analyses.  
869 ● To assess the statistical relationship between the variations in the EM rainfall  
870 amount, distribution and intensity, on the one hand, and the long-range  
871 variations of the characteristics of the air mass transport associated with the  
872 Indian Ocean Dipole, on the other hand.  
873  
874

875 **2.8.3. Future Research on African Monsoon Impacts on the Climate**  
876 **of the Mediterranean**  
877

- 878  
879 ● To study teleconnections between the summer climate in the Mediterranean  
880 and the African Monsoon by using numerical simulations. The major tools  
881 could be the NCEP–NCAR and ECMWF reanalyses, historical time series  
882 of atmospheric parameters in southern Europe (Luterbacher et al., this book),  
883 Regional numerical models, scenarios for future climate produced by global  
884 climate models, like the ones from the Canadian Centre for Climate Modelling  
885 and Analysis (CCCma), and also gridded precipitation data provided by the  
886 Global Precipitation Climatology Project.  
887 ● To perform numerical simulations with the Regional Model on different  
888 time-space scales for the domain including Europe, the Mediterranean  
889 Basin and the northern part of the African continent north to the Gulf of  
890 Guinea. The effects of SST variability in the Gulf of Guinea on the climate  
891 variability in the Mediterranean should be assessed by using an approach  
892 similar to that presented by Vizy and Cook (2001, 2002). In turn, the influence  
893 of the Mediterranean SST on climate variability in the North African region  
894 should be studied.  
895 ● To perform time-slice experiments for the future climate evolution by using the  
896 regional model, according to different available scenarios. Since the phenom-  
897 ena are embedded in the large scale circulation and in particular in the Hadley  
898 cell circulation, therefore a mathematical model of the evolution of the Hadley  
899 cell should be elaborated.  
900 ● To study the linkage between the Mediterranean climate, CLIVAR VACS  
901 (Variability of the African Climate System) and AMMA (African Monsoon  
902 Multidisciplinary Activities).

903 **2.8.4. Future Research on Tropical Intrusions into the Mediterranean Basin**

904

- 905 ● To define general mechanisms of tropical intrusions of the Red Sea trough and  
906 the tropical plume into the EM.  
907 ● To find out the role of the Red Sea trough and the tropical plume in the general  
908 atmospheric circulation over the Mediterranean. In particular, to find out their  
909 role in the transport of moisture and angular momentum.  
910 ● To study physical reasons and mechanisms of the recent increase in tropical  
911 intrusions into the Mediterranean.

912

913

914 **Acknowledgements**

915

916 The study in Tel Aviv University was supported by the GLOWA-Jordan River  
917 BMBF-MOS project.

918

919

920 **References**

921

922

923 R. Allan, J. Lindesay, and D. Parker, (Eds). *El Nino-Southern Oscillation and Climate*  
924 *Variability*. CSIRO Publishing, Collingwood, Victoria, Australia, 405 pp.

925 Alpert, P., & Ziv, B. (1989). The Sharav cyclone: observations and some theoretical  
926 considerations. *J. Geophys. Res.*, **94**, 18495–18514.

927 Alpert, P., Neeman, B. U., & Shay-El, Y. (1990). Intermonthly variability of cyclone  
928 tracks in the Mediterranean. *J. Climate*, **3**, 1474–1478.

929 Alpert, P., Stein, U., & Tsidulko, M. (1995). Role of sea fluxes and topography in  
930 Eastern Mediterranean cyclogenesis. *The Global Atmosphere-Ocean System*, **3**, 55–79.

931 Alpert, P., Ben-Gai, T., Baharad, A., Benjamini, Y., Yekutieli, D., Colacino, M.,  
932 Diodato, L., Ramis, C., Homar, V., Romero, R., Michaelides, S., & Manes, A. (2002).  
933 The paradoxical increase of Mediterranean extreme daily rainfall in spite of decrease in  
934 total values. *Geophys. Res. Lett.*, **29(11)**, 31-1–31-4, (June issue).

935 Alpert, P., Ilani, R., da-Silva, A., Rudack, A., & Mandel, M. (2003). Seasonal prediction  
936 for Israel winter precipitation based on northern hemispheric EOF. MERCHAVIM  
937 special issue for Prof. A. Bitan, in press.

938 Alpert, P., Osetinsky, I., Ziv, B., & Shafir, H. (2004a). Semi-objective classification for  
939 daily synoptic systems: application to the EM climate change. *Int. J. Climatol.*, **24**,  
940 1001–1011.

941 Alpert, P., Osetinsky, I., Ziv, B., & Shafir, H. (2004b). A new seasons definition based on  
942 the classified daily synoptic systems: an example for the EM. *Int. J. Climatol.*, **24**,  
943 1013–1021.

944 Alpert, P., Kishcha, P., Shtivelman, A., Krichak, S. O., & Joseph, J. H. (2004c). Vertical  
945 distribution of Saharan dust based on 2.5-year model predictions. *Atmos. Res.*, **70**,  
946 109–130.

947 Andersen, D. (1999). Extremes in the Indian Ocean. *Nature*, **401**, 337–339.

AQ: please update the status of  
the references which are in press, in  
preparation, submitted, in review etc.,  
if any in the reference list

AQ: please update the status of  
the references which are in press,  
in preparation, in review etc., if any  
in the reference list

- 944 Baldi, M., Crisci, A., Dalu, G. A., Maracchi, G., Meneguzzo, F. & Pasqui, M. (2002).  
945 Mediterranean climate and its connections to regional and global processes.  
946 *Proceedings of the First Italian IGBP Conference Mediterraneo e Italia nel*  
947 *Cambiamento Globale: un ponte fra scienza e societa' Paestum*, Salerno, 14–16  
948 November 2002.
- 948 Baldi, M., Capecchi, V., Crisci, A., Dalu, G. A., Maracchi, G., Meneguzzo, F. &  
949 Pasqui, M. (2003a). Mediterranean summer climate and its relationship to regional and  
950 global processes. *Proceedings of the Sixth European Conference on Applications of*  
951 *Meteorology*, Rome, 15–19 September 2003.
- 951 Baldi, M., Capecchi, V., Crisci, A., Dalu, G.A., Maracchi, G., Meneguzzo, F., &  
952 Pasqui, M. (2003b). Numerical analysis of the teleconnection of the West Africa  
953 monsoon with the mediterranean summer climate. *Environmental Fluid Mechanics*,  
954 submitted.
- 955 Barkan, J., Alpert, P., Kutiel, H., Kishcha, P. (2005). The synoptics of dust trans-  
956 portation days from Africa toward Italy and Central Europe. *Journal of Geophysical*  
957 *Research – Atmosphere*, in press.
- 957 Bergametti, G., Dutot, A. L., Buat-Menard, P., Losno, R., & Remoudaki, E. (1989).  
958 Seasonal variability of the elemental composition of atmospheric aerosol particles over  
959 the northwestern Mediterranean. *Tellus*, **41B**, 353–361.
- 960 Chen, J., Carlson, B. E., & Del Genio, A. D. (2002). Evidence for strengthening of the  
961 tropical general circulation in the 1990s. *Science*, **295**, 838–841.
- 961 Chou, C., & Neelin, J. D. (2003). Mechanisms limiting the northward extent of the  
962 northern summer monsoons over North America, Asia, and Africa. *J. Climate*, **16**,  
963 406–425.
- 964 Compo, G. P., Sardeshmukh, P. D., & Penland, C. (2001). Changes of subseasonal  
965 variability associated with El Niño. *J. Climate*, **14**, 3356–3374.
- 966 Curtis, S., & Hastenrath, S. (1995). Forcing of anomalous SST evolution in the tropical  
967 Atlantic during Pacific warm events. *J. Geophys. Res.*, **100**, 15835–15847.
- 968 Dayan, U., Ziv, B., Margalit, A., Morin, E., & Sharon, D. (2001). A severe autumn  
969 storm over the Middle-East: synoptic and mesoscale convection analysis. *Theor. Appl.*  
970 *Clim.*, **69**, 103–122.
- 970 Dima, I. M., & Wallace, J. M. (2003). On the seasonality of the Hadley Cell. *J. Atmos.*  
971 *Sci.*, **60**, 1522–1527.
- 972 Diaz, H. F., Hoerling, M. P., & Eischeid, J. K. (2001). ENSO variability, teleconnections  
973 and climate change. *Int. J. Climatol.*, **21**, 1845–1862.
- 974 Enfield, D. B., & Mayer, D. A. (1997). Tropical Atlantic SST variability and its relation  
975 to El Niño Southern Oscillation. *J. Geophys. Res.*, **102**, 929–945.
- 975 Fraedrich, K. (1994). ENSO Impact on Europe? - A Review. *Tellus*, **46A**, 541–552.
- 976 Fraedrich, K., & Müller, K. (1992). Climate anomalies in Europe associated with ENSO  
977 extremes. *Int. J. Climatol.*, **12**, 25–31.
- 978 Giorgi, F., (2002). Variability and trends of sub-continental scale surface climate  
979 in the twentieth century. Part I: observations. *Clim. Dyn.* doi: 10.1007/s00382-001-  
980 0204-x.
- 980 Gobbi, G. P., Barnaba, F., & Ammannato, L. (2004). The vertical distribution of  
981 aerosols, Saharan dust and clouds at Rome (Italy) in the year 2001. *Atmos. Chem.*  
982 *Phys.*, **3**, 2161–2172.
- 983 Griffies, S. M., & Bryan, K. (1997). Predictability of North Atlantic climate variability.  
984 *Science*, **275**, 181–184.

- 985 Gualdi, S., Navarra, A., Guilyardi, E., & Delecluse, P. (2003). The SINTEX coupled  
986 GCM. The tropical Indo-Pacific region. *Ann. Geophys.*, **46**, 1–26.
- 987 Halpert, M. S., & Ropelewski, C. F. (1992). Surface temperature patterns associated  
with the SO. *J. Climate.*, **5**, 577–593.
- 988 Hoerling, M. P., Hurrell, J. W., Xu, T., Bates, G. T., & Phillips, A. (2004). Twentieth  
989 century North Atlantic climate change. Part II: understanding the effect of Indian  
990 Ocean warming. *Clim. Dyn.*, **23**, 391–405, doi: 10.1007/s00382-004-0433-x.
- 991 Hoskins, B. J., & Berrisford, P. (1988). A potential vorticity perspective of the storm of  
992 15–16 October 1987. *Weather*, **42**, 122–129.
- 993 Huang, J., Higuchi, K., & Shabbar, A. (1998). The relationship between the North  
994 Atlantic Oscillation and the El Niño-Southern Oscillation. *Geophys. Res. Lett.*, **25**,  
2707–2710.
- 995 Hurrell, J. W., Hoerling, M. P., Phillips, A. S., & Xu, T. (2004). Twentieth century North  
996 Atlantic climate change. Part I: assessing determinism. *Clim. Dyn.*, **23**, 371–389, doi:  
997 10.1007/s00382-004-0432-y.
- 998 Kadioğlu, M., Tulunay, Y., & Borhan, Y. (1999). Variability of Turkish precipitation  
999 compared to El Niño events. *Geophys. Res. Lett.*, **26**, 1597–1600.
- 1000 Kahana, R., B. Ziv, Enzel, Y., & Dayan, U. (2002). Synoptic climatology of major floods  
in the Negev Desert, Israel. *Int. J. Clim.*, **22**, 822–867.
- 1001 Kiladis, G. N., & Díaz, H. F. (1989). Global climatic anomalies associated with extremes  
1002 in the Southern Oscillation. *J. Climate*, **2**, 1069–1090.
- 1003 Kishcha, P., Barnaba, F., Gobbi, G. P., Alpert, P., Shtivelman, A., Krichak, S. O., &  
1004 Joseph, J. H. (2005). Vertical distribution of Saharan dust over Rome (Italy):  
1005 Comparison between 3-year model predictions and lidar soundings. *J. Geophys. Res.*,  
**110**, doi:10.1029/2004JD005480, in press.
- 1006 Klein, S. A., Soden, B. J., & Lau, N.-C. (1999). Remote sea surface temperature variations  
1007 during ENSO: evidence for a tropical atmospheric bridge. *J. Climate*, **12**, 917–932.
- 1008 Knippertz, P., Fink, A. H., Reiner, A., & Speth, P. (2003). Three late summer/early  
1009 autumn cases of tropical-extratropical interactions causing precipitation in Northwest  
Africa. *Mon. Wea. Rev.*, **131**, 116–135.
- 1010 Krichak, S. O., Alpert, P., & Dayan, M. (2004). The role of atmospheric processes  
1011 associated with hurricane Olga in the December 2001 floods in Israel. *J.*  
1012 *Hydrometeorology*, **5**(6), 1259–1270.
- 1013 Krichak, S. O., Alpert, P., & Krishnamurti, T. N. (1997a). Interaction of topography  
1014 and tropospheric flow - a possible generator for the Red Sea trough? *Meteorol.*  
*Atmosph. Phys.*, **63**(3–4), 149–158.
- 1015 Krichak, S. O., Alpert, P., & Krishnamurti, T. N. (1997b). Red Sea trough/cyclone  
1016 development - numerical investigation. *Meteorol Atmosph. Phys.*, **63**(3–4), 159–170.
- 1017 Krichak, S. O., & Alpert, P. (1998). Role of large scale moist dynamics in November 1-5  
1018 1994 hazardous Mediterranean Weather, **103**(D16), 19453–19468.
- 1019 Kripalani, R. H., & Kulkarni, A. (1999). Climatology and variability of historical Soviet  
1020 snow depth data: some new perspectives in snow – Indian monsoon teleconnections.  
*Clim. Dyn.*, **15**, 475–489.
- 1021 Laita, M., & Grimalt, M. (1997). Vorticity and pressure anomalies in the western  
1022 Mediterranean during El Niño/Southern Oscillation extremes. *Int. J. Climatol.*, **17**,  
1023 475–482.
- 1024 Lanzante, J. R. (1996). Lag relationships involving tropical sea surface temperatures.  
1025 *J. Climate*, **9**, 2568–2578.

- 1026 Lau, N.-C., & Nath, M. J. (1996). The role of the 'atmospheric bridge' in linking tropical  
1027 Pacific ENSO events to extratropical SST anomalies. *J. Climate*, **9**, 2036–2057.
- 1028 Lau, N.-C., & Nath, M. J. (2001). Impact of ENSO on SST variability in the North  
1029 Pacific and North Atlantic: seasonal dependence and role of extratropical sea-air  
1030 coupling. *J. Climate*, **14**, 2846–2866.
- 1031 Liu, X., & Yanai, M. (2001). Relationship between the Indian monsoon rainfall and the  
1032 tropospheric temperature over the Eurasian continent. *Quart. J. Roy. Met. Soc.*, **127**,  
1033 909–938.
- 1034 Lloyd-Hughes, B., & Saunders, M. A. (2002). Seasonal prediction of European spring  
1035 precipitation from El Niño-Southern Oscillation and local sea-surface temperatures.  
1036 *Int. J. Climatol.*, **22**, 1–14.
- 1037 Loon, H., & Madden, R. A. (1981). The Southern Oscillation. Part I: global associations  
1038 with pressure and temperature in Northern winter. *Mon. Wea. Rev.*, **109**, 1150–1168.
- 1039 Mariotti, A., Zeng, N., & Lau, K. M. (2002). Euro-Mediterranean rainfall and ENSO – a  
1040 seasonally varying relationship. *Geophys. Res. Lett.*, **29**, doi 10.1029/2001GL014248.
- 1041 Mariotti, A., Ballabrera-Poy, J., & Zeng, N. (2005). Tropical influence on Euro-Asian  
1042 autumn rainfall variability. *Clim. Dyn.*, **24**(5), 511–521, 10.1007/s00382-004-0498-6.
- 1043 Merkel, U., & Latif, M. (2002). A high resolution AGCM study of the El Niño impact  
1044 on the North Atlantic/European sector. *Geophys. Res. Lett.*, **29**(9), 1291.
- 1045 Mason, S. J., & Goddard, L. (2001). Probabilistic precipitation anomalies associated  
1046 with ENSO. *Bulletin of the Americ. Meteorol. Soc.*, **82**(4), 619–638.
- 1047 Mestas-Nunez, A. M., & Enfield, D. B. (2001). Eastern Equatorial Pacific SST  
1048 variability: ENSO and non-ENSO components and their climatic associations. *J.*  
1049 *Climate*, **14**, 391–402.
- 1050 Moron, V., & Ward, M. N. (1998). ENSO teleconnections with climate variability in the  
1051 European and African sectors. *Weather*, **53**, 287–295.
- 1052 Moulin, C., Lambert, C., Dayan, U., Masson, V., Ramonet, M., Bousquet, P.,  
1053 Legrand, M., Balkanski, Y., Guelle, W., Marticorena, B., Bergametti, G., & Dulac, F.  
1054 (1998). Satellite climatology of African dust transport in the Mediterranean  
1055 atmosphere. *J. Geophys. Res.*, **103**, 13137–13144.
- 1056 Nobre, P., & Shukla, J. (1996). Variations of SST, wind stress, and rainfall over the  
1057 tropical Atlantic and South America. *J. Climate*, **9**, 2464–2479.
- 1058 Oldenborgh, G. J., Burgers, G., & Klein-Tank, A. (2000). On the El Niño teleconnection  
1059 to spring precipitation in Europe. *Int. J. Climatol.*, **20**, 565–574.
- 1060 Parthasarathy, B., Munot, A. A., & Kothawale, D. R. (1995). Monthly and seasonal  
1061 rainfall series for all-India homogeneous regions and meteorological subdivisions:  
1062 1871–1994. Contributions from Indian Institute of Tropical Meteorology. Research  
1063 Report RR-065, Aug. 1995, Pune, India.
- 1064 Pozo-Vázquez, D., Esteban-Parra, M. J., Rodrigo, F. S., & Castro-Diez, Y. (2001). The  
1065 association between ENSO and winter atmospheric circulation and temperature in  
1066 the North Atlantic region. *J. Climate*, **14**, 3408–3420.
- Price, C., Stone, L., Rajagopalan, B., & Alpert, P. (1998). A possible link between  
El Niño and precipitation in Israel. *Geophys. Res. Lett.*, **25**, 3963–3966.
- Raicich, F., Pinardi, N., & Navarra, A. (2003). Teleconnections between Indian  
Monsoon and Sahel rainfall and the Mediterranean. *Int. J. Climatol.*, **23**, 173–186.
- Reale, O., Feudale, L., & Turato, B. (2001). Evaporative moisture sources  
during a sequence of floods in the Mediterranean region. *Geophys. Res. Lett.*, **28**,  
2085–2088.

- 1067 Reddaway, J. M., & Bigg, G. R. (1996). Climatic change over the Mediterranean and  
1068 links to the more general atmospheric circulation. *Int. J. Climatol.*, **16**, 651–661.
- 1069 Rocha, A. (1999). Low-frequency variability of seasonal rainfall over the Iberian  
1070 Peninsula and ENSO. *Int. J. Climatol.*, **19**, 889–901.
- 1071 Rodó, X. (2001). Reversal of three global atmospheric fields linking changes in SST  
1072 anomalies in the Pacific, Atlantic and Indian oceans at tropical latitudes and  
1073 midlatitudes. *Clim. Dyn.*, **18**, 203–217.
- 1074 Rodó, X., & Comin, F. A. (2000). Links between large-scale anomalies, rainfall and wine  
1075 quality in the Iberian Peninsula during the last three decades. *Global Change Biology*,  
1076 **6**(3), 267–273.
- 1077 Rodó, X., Baert, E., & Comín, F. A. (1997). Variations in seasonal rainfall in Southern  
1078 Europe during the present century: relationships with the NAO and the ENSO. *Clim.*  
1079 *Dyn.*, **13**, 275–284.
- 1080 Rodó, X., Pascual, M., Fuchs, G., & Faruque, A. S. G. (2002). ENSO and cholera: a  
1081 nonstationary link related to climate change? *PNAS*, **99**, 12901–12906.
- 1082 Rodríguez-Arias, M. A., & Rodó, X. (2003). A primer on the study of transitory dynamics  
1083 in ecological series using the scale-dependent correlation analysis. *Oecologia*, in press.
- 1084 Rodríguez-Puebla, C., Encinas, A. H., Nieto, S., & Garmendia, J. (1998). Spatial  
1085 and temporal patterns of annual precipitation variability over the Iberian Peninsula.  
1086 *Int. J. Climatol.*, **18**, 299–316.
- 1087 Rodwell, M. J., & Hoskins, B. J. (1996). Monsoons and the dynamic of deserts. *Quar.*  
1088 *J. Roy. Meteorol. Soc.*, **122**, 1385–1404.
- 1089 Rodwell, M. J., & Hoskins, B. J. (2001). Subtropical anticyclones and summer monsoons.  
1090 *J. Climate*, **14**, 3192–3211.
- 1091 Ropelewski, C. F., & Halpert, M. S. (1987). Global and regional precipitation patterns  
1092 associated with El Niño-Southern Oscillation. *Mon. Wea. Rev.*, **115**, 1606–1626.
- 1093 Rowell, D. P. (2003). The impact of Mediterranean SSTs on the Sahelian rainfall season.  
1094 *J. Climate*, **16**, 849–862.
- 1095 Ruiz-Barradas, A., Carton, J. A., & Nigam, S. (2003). Role of the atmosphere in climate  
1096 variability of the tropical Atlantic. *J. Climate*, **16**, 2052–2065.
- 1097 Saaroni, H., Bitan, A., Alpert, P., & Ziv, B. (1996). Continental outbreaks into the  
1098 Levant and Eastern Mediterranean. *Int. J. Clim.*, **16**, 1–17.
- 1099 Saaroni, H., Ziv, B., Edelson, J., & Alpert, P. (2003). Long-term variations in summer  
1100 temperatures over the Eastern Mediterranean. *Geo. Res. Lett.*, **30**(18), 1946,  
1101 doi:10.1029/2003GL017742.
- 1102 Saji, N. H., Goswami, B. N., Vinayachandran, P. N., & Yamagata, T. (1999). A dipole  
1103 mode in the tropical Indian Ocean. *Nature*, **401**, 360–363.
- 1104 Saravanan, R., & Chang, P. (2000). Interaction between tropical Atlantic variability and  
1105 ENSO. *J. Climate*, 2177–2194.
- 1106 Stein, U., & Alpert, P. (2003). Factor separation in numerical simulations. *J. Atmos. Sci.*,  
1107 **50**, 2107–2115.
- 1108 Subbaramayya, I., Vivekanandababu, S., & Naidu, C. V. (1990). Variations in the onset  
1109 of the Indian south-west monsoon and summer circulation anomalies. *Meteorol.*  
1110 *Magaz.*, **119**, 61–67.
- 1111 Sultan, B., & Janicot, S. (2000). Abrupt shift of the ITCZ over West Africa. *Geophys.*  
1112 *Res. Letter*, **27**, 3353–3356.
- 1113 Sultan, B., & Janicot, S. (2003). The West African monsoon dynamics. Part II the pre-  
1114 onset and the onset of the summer monsoon. *Journal of Climate*, in press.

AQ:  
please  
cite the  
reference

- 1108 Sutton, R. T., Jewson, S. P., & Rowell, D. P. (2000). The elements of climate variability  
1109 in the tropical Atlantic region. *J. Climate*, **13**, 3261–3284.
- 1110 Timmermann, A., Oberhuber, J., Bacher, A., Esch, M., Latif, M., & Roeckner, E.  
1111 (1999). Increase El Niño frequency in a climate model forced by future greenhouse  
1112 warming. *Nature*, **398**, 694–697.
- 1113 Trenberth, K. E., & Hoar, T. J. (1997). El Niño and climate change. *Geophys. Res. Lett.*,  
1114 **24**, 3057–3060.
- 1115 Trenberth, K. E., Branstator, W., Karoly, D., Kumar, A., Lau, N., & Ropelewski, C.  
1116 (1998). Progress during TOGA in understanding and modeling global teleconnections  
1117 associated with tropical sea surface temperatures. *J. Geophys. Res.*, **103**, 14291–14324.
- 1118 Türkes, M. (1998). Influence of geopotential heights, cyclone frequency and southern  
1119 oscillation on rainfall variations in Turkey. *Int. J. Climatol.*, **18**, 649–680.
- 1120 Vizy, E. K., & Cook, K. H. (2001). Mechanisms by which Gulf of Guinea and Eastern  
1121 North Atlantic sea surface temperature anomalies can influence African rainfall. *J.*  
1122 *Climate*, **11**, 3167–3191.
- 1123 Vizy, E. K., & Cook, K. H. (2002). Development and application of a mesoscale climate  
1124 model for the tropics: influence of sea surface temperature anomalies on the West  
1125 African monsoon. *J. Geophys. Res.*, 107(D3), 10.1029/2001JD000686.
- 1126 Wallace, J. M., & Gutzler, D. (1981). Teleconnections in the geopotential height fields  
1127 during the Northern Hemisphere winter. *Mon. Wea. Rev.*, **109**, 784–812.
- 1128 Webster, P., Moore, J. A. M., Loschnigg, J. P., & Leben, R. R. (1999). Coupled ocean  
1129 atmosphere dynamics in the Indian Ocean during 1997–98. *Nature*, **401**, 356–360.
- 1130 Wuethrich, B. (1995). El Niño goes critical. *New Scientist*, **4**, (Feb), 32–35.
- 1131 Xoplaki, E. (2002). Climate variability in the Mediterranean. Ph.D. thesis, University of  
1132 Bern, Switzerland, [http://sinus.unibe.ch/klimet/docs/phd\\_xoplaki.pdf](http://sinus.unibe.ch/klimet/docs/phd_xoplaki.pdf).
- 1133 Yakir, D., Lev-Yadun, S., & Zangvil, A. (1996). El Niño and tree growth near Jerusalem  
1134 over the last 20 years. *Global Change Biology*, **2**, 101–105.
- 1135 Zangvil, A., & Isakson, A. (1995). Structure of the water vapor field associated with an  
1136 early spring rainstorm over the Eastern Mediterranean. *Isr. J. Earth Sci.*, **44**, 159–168.
- 1137 Ziv, B. (2001). A subtropical rainstorm associated with a tropical plume over Africa and  
1138 the Middle-East. *Theor. Appl. Clim.*, **69**(1/2), 91–102.
- 1139 Ziv, B., Saaroni, H., & Alpert, P. (2004a). The factors governing the summer regime of  
1140 the Eastern Mediterranean. *Int. J. Clim.*, **24**, 1859–1871.
- 1141 Ziv, B., Dayan, U., & Sharon, D. (2004b). A mid-winter, tropical extreme flood-  
1142 producing storm in southern Israel: synoptic scale analysis. *Meteorology and*  
1143 *Atmospheric Physics*, doi, 10.1007/s00703-003-0054-7.
- 1144  
1145  
1146  
1147  
1148